Nuclear Instruments and Methods in Physics Research A 355 (1995) 624-631

ELSEVIER

NUCLEAR INSTRUMENTS & METHODS IN PHYSICS RESEARCH Section A

A cosmic-ray veto system for the gravitational wave detector NAUTILUS

E. Coccia [b], A. Marini [a], G. Mazzitelli [a], G. Modestino [a], F. Ricci [c], F. Ronga [a], L. Votano [a,*]

[a] *Laboratori Nazionali di Frascati, Istituto Nazionale di Fisica Nucleare (INFN), P.O. Box 13, I-00044 Frascati, Italy*

[b] *Università di Roma II, e Istituto Nazionale di Fisica Nucleare (INFN), Sez. di Roma II, Tor Vergata, Via Orazio Raimondo, I-00173 Roma, Italy*

[c] *Università di Roma La Sapienza, e Istituto Nazionale di Fisica Nucleare (INFN), Sez. di Roma I, La Sapienza, piazzale Aldo Moro 2, I-00185 Roma, Italy*

Received 30 May 1994; revised form received 15 September 1994

Abstract

The ultracryogenic resonant gravitational wave antenna NAUTILUS now operating at Frascati INFN National Laboratory has been provided with a cosmic-ray veto system consisting of layers of streamer tubes. The experimental setup and performance of the system are shown. Preliminary results on the data collected during the calibration operations of the antenna are also presented together with the expected number of events from the interactions of high-energy hadrons and muons and multihadron showers with the gravitational antenna.

1. Introduction

NAUTILUS [1] is a new-generation ultracryogenic resonant gravitational wave antenna in operation at Frascati INFN National Laboratory. The goal of the antenna is to detect bursts of gravitational waves from sources located at distances up to the Virgo Cluster of galaxies. In order to clearly assign the signal detected by the antenna to g.w. bursts, the usual strategy is to make coincidences among similar detectors and to use local seismic and electromagnetic veto systems. In addition, the NAUTILUS detector has been equipped with a cosmic-ray veto system consisting of layers of streamer tubes [2] placed above and below the antenna cryostat.

The pioneering contribution to the study of the influence of high-energy particles on gravitational wave antennas was given in the sixties by Beron et al. at Stanford [3,4], while ten years later, Grassi Strini et al. [5] found a quantitative relation between the particle energy loss and the vibrational energy measured in an aluminum bar, using a 30-MeV proton beam. A plastic scintillator cosmic-ray telescope [6] was in operation at Stanford together with the cryogenic antenna in 1986, but no signals were found over the detector noise of about 20 mK. Amaldi and Pizzella [7], and then Ricci [8], calculated and simulated the energy loss distribution of high-energy cosmic muons crossing a Weber-type antenna and derived the expected number of events giving a signal over a prefixed threshold. Recently, Chiang et al. [9] have published results of a Monte Carlo simulation of the interaction of cosmic-ray hadrons with a resonant gravitational wave antenna.

The expected sensitivity of NAUTILUS is one order of magnitude better than that of other similar detectors; at the effective noise temperature T_{eff} of about 1 mK, we expect a few events per day originated by cosmic rays, which will give a detectable signal in the antenna, thus requiring a cosmic-ray monitor. In addition, the possibility of obtaining a coincidence between cosmic-ray detection and energy oscillation of the bar can lead to information on the sensitivity of a large aluminum bar (2300 kg) when used as a particle detector of rare events in cosmic rays [10].

In this paper we report the experimental setup and the preliminary results on the data from the cosmic-ray detector assembled for NAUTILUS. We also give the number of events expected from the interaction of high-energy hadrons and muons with the bar and evaluate the effect due to multihadron showers for the first time. For the simulation we have used a relation between the vibrational energy of the antenna and the energy lost by incident particles, improved with parameters suitable for low temperatures.

2. Cosmic-ray monitor for the NAUTILUS gravitational wave detector

The cosmic-ray detector has been designed in order to optimize the detection acceptance for high-energy particles and extensive air showers (EAS) interacting with the antenna. It has a modular structure that facilitates disassembly during the gravitational wave detector maintenance operations.

* Corresponding author.

0168-9002/95/$09.50
SSDI 0168-9002(94)01166-4

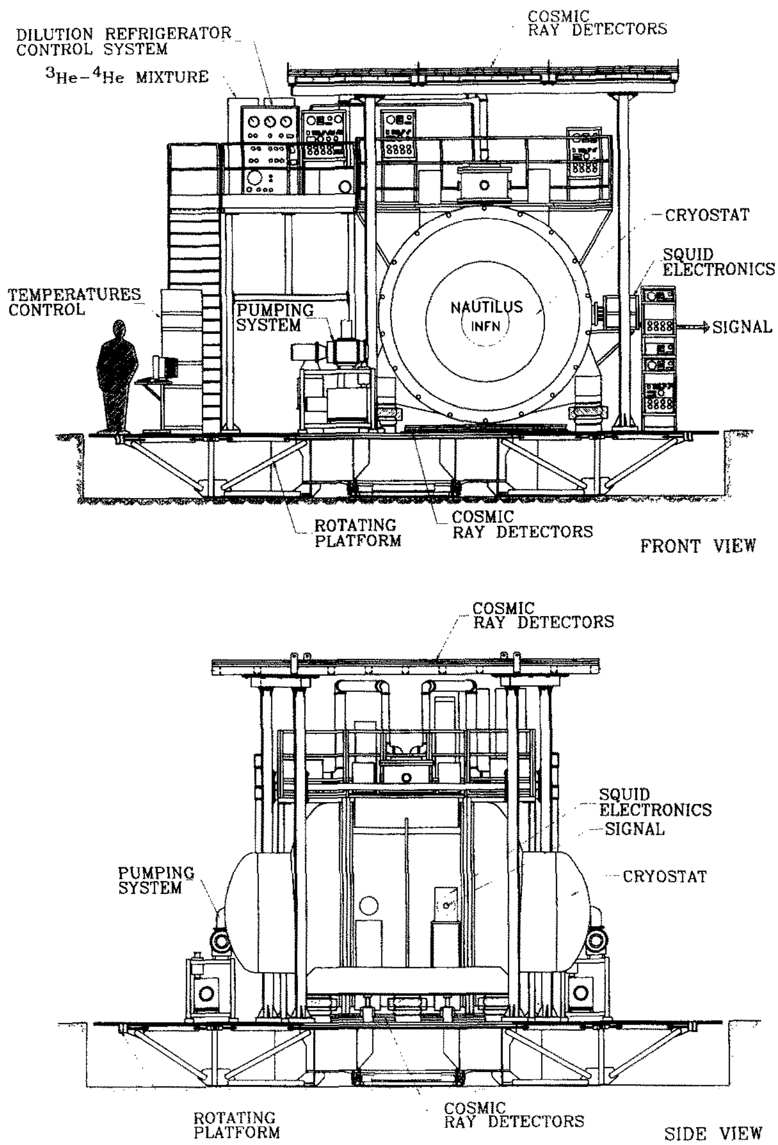

Fig. 1. Layout of the NAUTILUS antenna.

In implementing the cosmic-ray detector, we have been limited by the space left available by the cryostat. The detector consists of seven layers of limited streamer tubes (LSTs), three (6×6 m^2, 24 LSTs each) mounted above the cryostat (at a distance of 3.95 m from the antenna center) and four layers (6×2.75 m^2, 11 LSTs each) placed at ground level (see Fig. 1). The analog readout of the LST wires allows a measurement of the multiplicity of the particles impinging on the detector.

The LSTs are 6.0-m-long large-size coverless plastic tubes (similar to those of the MACRO experiment [11]) operating in the limited streamer regime. Each tube consists of eight PVC-open-profile rectangular cells with a cross section of 3×3 cm^2 and coated with graphite ($R \simeq 1$–2 k$\Omega/\square$). A Cu-Be 100-μm-diam anode wire is strung along the center of each cell; it is supported every 50 cm by plastic bridges and connected through a printed circuit board to a common high-voltage bus. The profiles are inserted in an uncoated PVC sleeve. Plastic caps welded at the ends provide electrical and gas connections. The performance of these detectors as a function of HV and different gas mixtures has been described elsewhere [12]. We have intensively tested each tube against electrical failures and gas leakages in order to ensure very stable operating conditions for the whole system. The tubes are continuously fluxed with a 60% isobutane and 40% Ar gas mixture. This high-quenched mixture

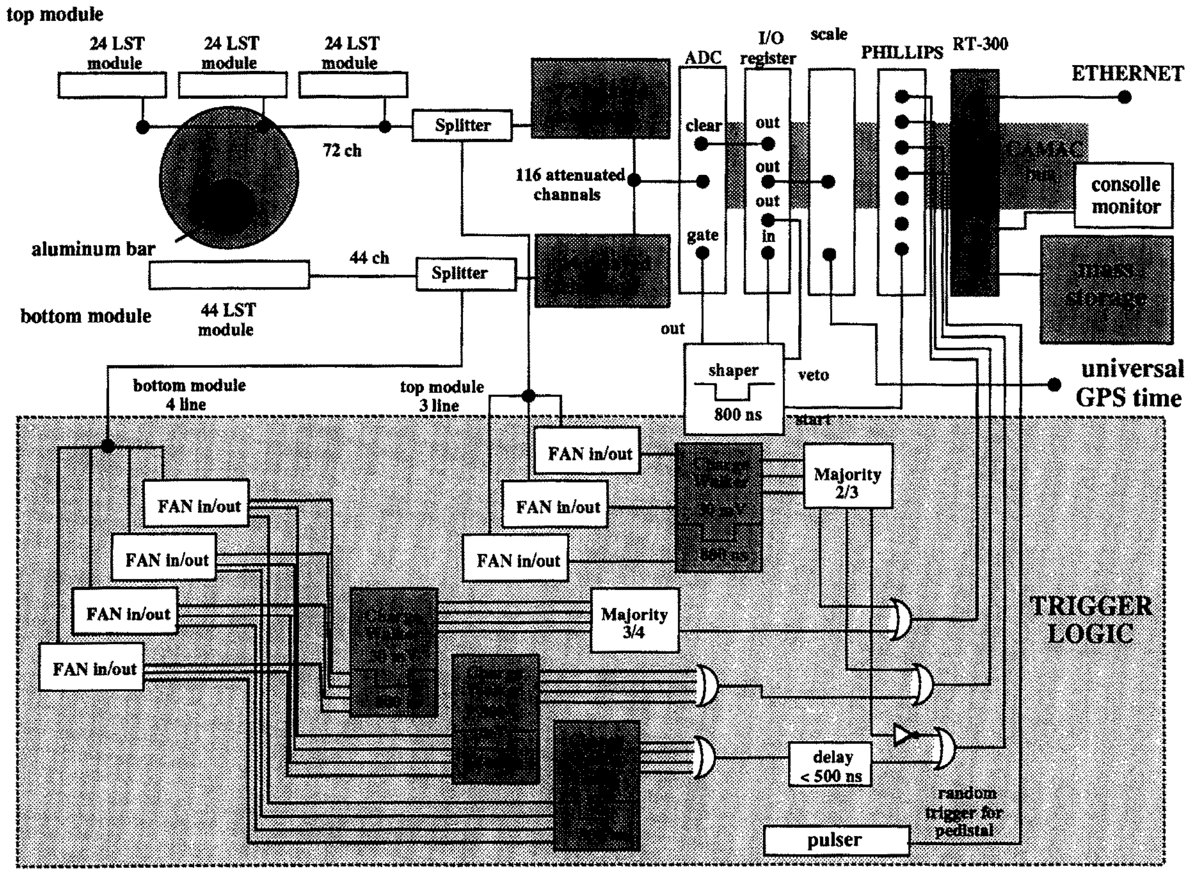

Fig. 2. Readout system.

ensures a low number of after-pulses, thus providing a better resolution in the particle multiplicity measurement. The tubes are operated at 5550 V; at this value the single streamer charge has an average value of 60 pC.

A schematic of the readout system is shown in Fig. 2. Signals from the eight wires of one tube are OR-ed together and each of these outputs is split into two signals: the first one is sent to the trigger logic, while the second is attenuated (about 70 times), delayed by 500 ns, and then processed by a 32-channel-ADC 12 bits (CAEN C205). The ADC gate signal is provided by the OR of the selected triggers. A typical charge distribution for muons is showed in Fig. 3. The charge peak has been set at about 4 ADC channels in order to have a large dynamic range for showers. Therefore, the ADC saturation threshold is approximately equivalent to 1000 particles.

The trigger logic is designed for detection of high-energy muons and hadrons interacting in the antenna or EAS. The analog signals of the streamer tubes belonging to the same layer are OR-ed together, and the seven outputs are fed into a NIM module (Charge Walker) developed at the Frascati Laboratory. It consists of a 4-channel charge integrator with autoreset at 500 ns (corresponding to the maximum drift time in the tube), which provides an analog output

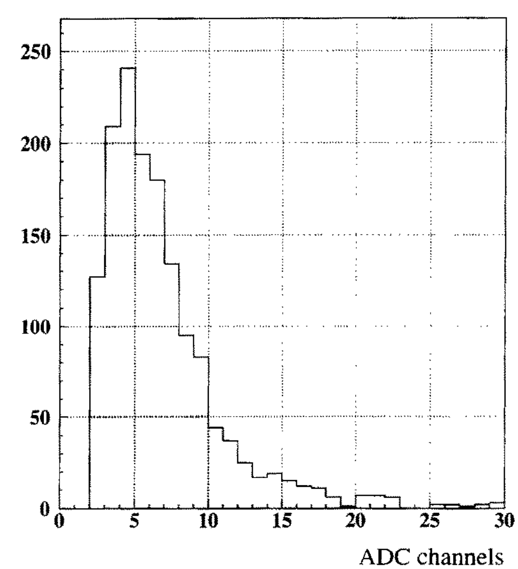

Fig. 3. A typical muon charge distribution.

(1 mV/pC) and a logical signal from a comparator with a preset threshold. The width of the output signal and the threshold can be set. The threshold applied to the seven layer signals is then linearly related to the particle multiplicity detected on the relative layer.

Three different triggers can be selected:

The first trigger (or μ trigger) is used for a periodic calibration of the system. We require the coincidence of at least two layers on the top module and three layers on the bottom; the thresholds are set to the single particle level (30 mV). The measured rate of events is about 600 Hz.

The second trigger (or interacting particle trigger) selects those events in which one or more particles interact with the gravitational wave detector. Thus, we require one or more particles in at least two layers of the top module and ten or more particles in the four layers of the bottom module. The rate of this trigger is about 2 Hz.

The third trigger (or neutral particle trigger) requires that no particles cross the top module, and that more than 20 particles cross the bottom module (the rate is about 2 Hz). This trigger should detect neutrons interacting in the bar or the large-angle charged particles that do not cross the upper telescope. Moreover, we periodically use a random trigger in order to determine the ADC channel pedestals.

Data acquisition is performed by a Kinetic Systems VANTAGE 300 intelligent crate controller operating in the CAMAC environment and built around the Digital Equipment rtVAX 300 processor. VANTAGE 300 runs the DEC VAXELN operating system [13], which is optimized for real-time operations. A 16-channel-I/O REGISTER (CAEN C219) controls the ADC gates and is used for providing CLEAR signals and the veto logic. The acquisition throughput on mass storage is of the order of 450 Kbytes/day with a dead time of about 4%.

3. Monte Carlo simulation of the cosmic-ray effects

A full simulation of the interaction of single hadrons and muons with the NAUTILUS bar has been performed by improving an existing simulation [8] based on the GEANT3 package [14].

The energy lost by a cosmic ray is converted into a local expansion of the bar due to the growth of the temperature. The relation between particle energy loss and the innovation of the vibrational energy of the bar [15,16] can be described as follows:

$$E_n = kT_{\mathrm{eff}} =$$
$$\frac{4k}{9\pi}\frac{\gamma^2}{\rho L v^2}\left(\frac{\mathrm{d}E}{\mathrm{d}x}\right)^2\left[\sin\left(n\frac{\pi z}{L}\right)\frac{\sin\left(n\frac{\pi l_0\cos(\theta)}{2L}\right)}{n\frac{\pi R\cos(\theta)}{L}}\right]^2, \quad (1)$$

where (see Fig. 4) E_n is the energy change deposited in the nth vibrational mode, T_{eff} is the minimum energy detectable expressed in Kelvin, often used as measurement of

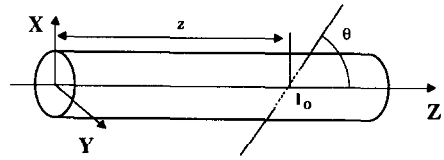

Fig. 4. Definition of geometrical parameters.

the detector sensitivity, $k = 8.63 \times 10^{-11}$ [MeV/K] is the Boltzmann constant, $\gamma = 1.6$ is the value of the Gruneisen constant at low temperature, $\rho = 2790$ [kg/m^3] is the Al 5056 density at low temperature, $v = 5400$ [m/s] is the Al 5056 sound speed at low temperature, $L = 3$ m is the length of the bar, l_0 is the path length of the particle in the bar, z is the coordinate measured with respect to the major axis Z of the bar, $R = 0.3$ m is the radius of the bar, θ is the angle of the incident particle with respect to the major axis Z of the bar, $\mathrm{d}E/\mathrm{d}x$ is the energy released by the particle in a unit of path length expressed in [GeV/m].

We have used the value measured at 1 K [17] for the Gruneisen constant. As far as we know no measurements exist at the operating temperature of the NAUTILUS; moreover, the effect of the passage of cosmic rays in a superconducting medium could require further experimental investigation.

The gravitational wave excites only the odd vibrational mode as a consequence of its quadrupolar nature. On the other hand, the interacting particle can be detected also on the second longitudinal mode [9], (see relation (1)). In Fig. 5 the bar response for the first and second harmonics due to a 1-GeV cosmic ray is shown.

The simulated geometrical structure is shown in Fig. 6; it includes the aluminum cylindrical bar, (radius 30 cm, length 300 cm), an iron cylindrical tube (4 cm thick, inner radius 34 cm, length 400 cm) that represents the vacuum can, two coaxial iron tubes (respectively 10 cm and 5 cm thick, 38.5 and 66 cm inner radius, 26.5 and 57.5 cm length) representing the equivalent thickness of the three copper shields and, finally, two iron disks (5 cm thick, 90.5 cm inner radius, 152 cm outer radius) placed at ± 85 cm from the antenna center in order to account mainly for the equivalent thickness of the cryostat massive rings. A vacuum box placed under the cryostat simulates the streamer tube layers.

In the evaluation of the expected numbers of detectable interactions of cosmic rays with the bar as a function of its sensitivity, a major role is played by hadron interactions. The hadron generator uses two different parametrizations for the experimental data: for hadrons with energy greater than 300 GeV, we have used the differential vertical spectrum at sea level given by Sihoan et al. [18] shown in Fig. 7 (single charged hadrons) up to a maximum energy of 10 TeV:

$$\frac{\mathrm{d}N}{\mathrm{d}E} = 1 \times 10^{-10}\left(\frac{E}{300}\right)^{-2.6} \quad [\mathrm{hadrons/(s\,cm^2\,sr\,GeV)}].$$

Below this energy, we have used the Arvela et al. [19]

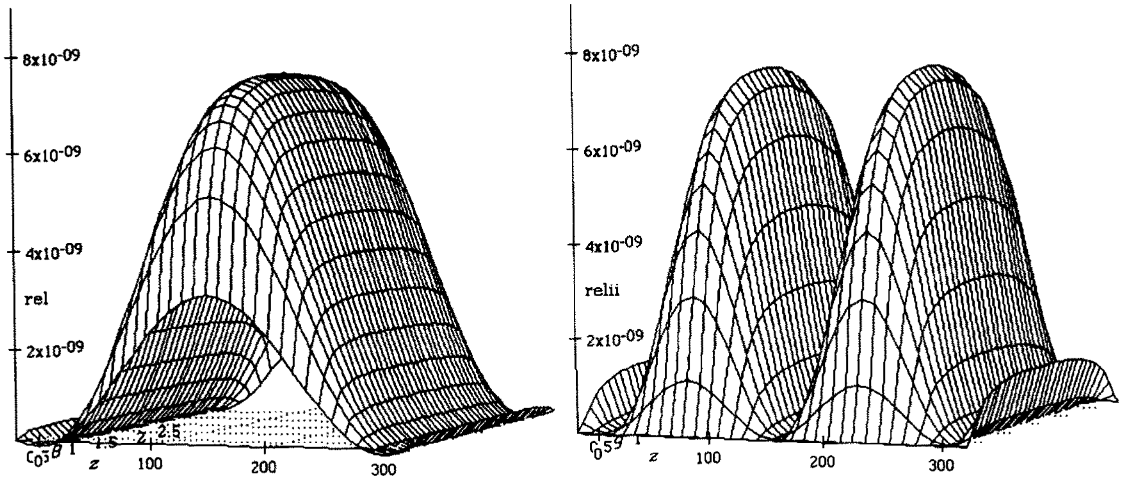

Fig. 5. Harmonics response as a function of the impinging particle angle and point.

parametrization with a minimum energy cut of 1 GeV:

$$\frac{dN}{dE} = 3 \times 10^{-4}\, E^{-2.5} \qquad [\text{hadrons}/(\text{s cm}^2\, \text{sr GeV})]\,.$$

A factor of $\exp(-h/\Lambda_N)$, where h is the atmospheric depth crossed by the particle and $\Lambda_N \simeq 140$ [g/cm^2], accounts for the hadron angular distribution. A 1.25 factor was also introduced, as suggested by Cowan et at. [20], to evaluate the hadron growth rate due to neutrons. The muon interaction contribution has been evaluated using, for the flux, the theoretical estimation of Dar [21] shown in Fig. 8, which is in good agreement with the available experimental data and a μ^+/μ^- charge ratio of 1.25.

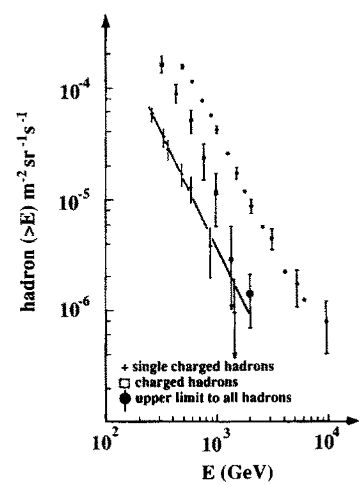

Fig. 7. Hadron flux from Sihoan et al. [18].

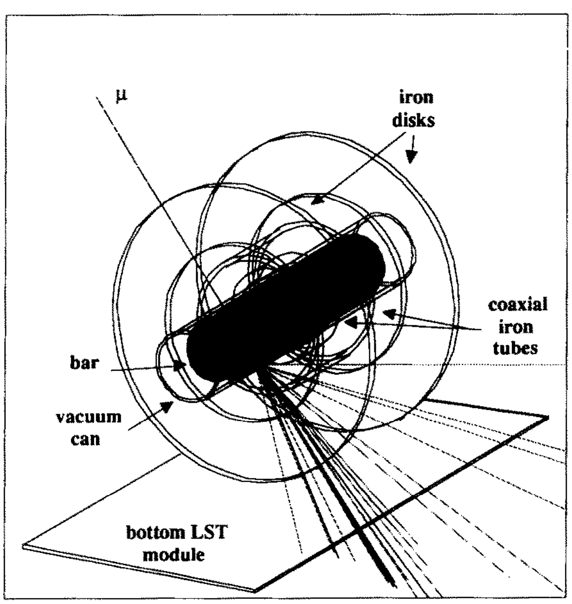

Fig. 6. Simulated interaction of a 1-TeV muon in the detector.

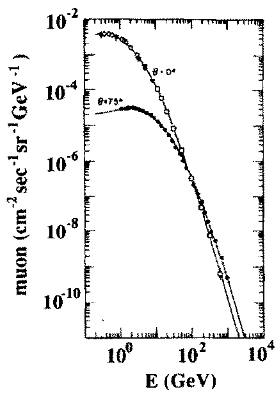

Fig. 8. Muon flux estimation from Dar [21].

Table 1
Expected event rate per day

Effective temperature [K]	Events/day [muons]	Events/day [hadrons]	Events/day [EAS]	Events/day [multi had.]	Events/day [total]
10^{-7}	1540	3310	137	-	4990
10^{-6}	155	463	35	-	653
10^{-5}	12.7	55.7	7	5.5	81
10^{-4}	1.2	6.2	1.3	3.7	12.3
10^{-3}	0.18	0.56	0.24	1.2	2.2
10^{-2}	0.002	0.035	0.04	0.1	0.2

Particle interaction and tracking in the detector has been performed using the GEANT 3.15 package, including the GEISHA simulator for the interaction of the hadrons in a shower. We have used the default energy cut values for secondary particles with the only exception being the kinetic energy cut for delta rays set to 100 KeV. The appropriate corrections are applied to the particle fluxes to account for zenith angle distribution and the NAUTILUS location. Fig. 9 gives the results on the expected number of events per day both from hadrons and muons as a function of the minimum energy released in the bar and the related minimum vibrational energy change detectable by the gravitational detector, measured in kelvin. Also reported are an analytical estimation of the contribution due to EAS, as suggested by Amaldi and Pizzella [7], and an estimation of multiple hadron events based on the Arvela et al. [19] Monte Carlo results. They evaluated the flux of multihadron showers ($N \geq 10$) with a total energy greater than 1000 GeV as a function of the detector area. For a 1-m^2 detector such as the NAUTILUS bar, the rate is the same as that of a single hadron with energy greater than 1000 GeV. Using the calculated distribution of the energy released in the bar by a hadron with a minimum energy of 100 GeV, we then evaluated the contribution of ten hadrons with the same minimum energy.

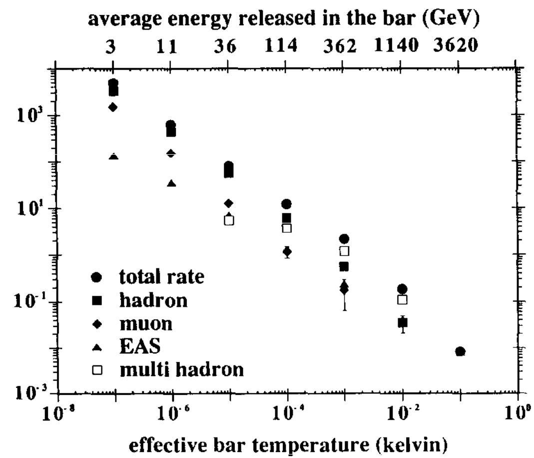

Fig. 9. Expected event rate per day.

At the sensitivity (about 30×10^{-3} K) already reached in the first run of NAUTILUS, we expect a total of a few detectable events per day; with the planned sensitivity of 100 μK, 10 events per day. (See also Table 1.)

We would like to stress that there is a lack of experimental information on the flux of single and multihadrons at high energy and that our evaluation is based on measurements of the hadron rate up to 2×10^3 GeV and affected by large errors.

In Fig. 10 we show the expected detection efficiency for hadron and muon interaction events, at fixed values of the minimum energy released in the bar, as a function of the particle multiplicity detected in the bottom module. In the Montecarlo simulation, we included the correct angular distribution; we did not require the crossing of the upper plane (as in the third trigger). We clearly have a correlation between the measured charge particle multiplicity and the cut on the minimum energy released in the bar.

4. Detector performance and calibration

In July 1993 a first cooling of NAUTILUS equipped with the cosmic-ray detector was effected and the calibration of the gravitational wave antenna started; data from the cosmic-ray detector were collected during this period.

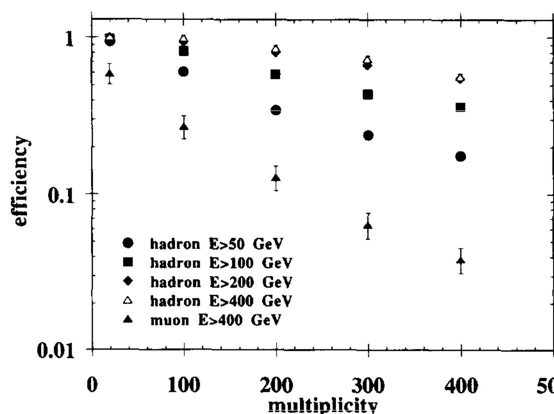

Fig. 10. Detection efficiency as a function of multiplicity cut.

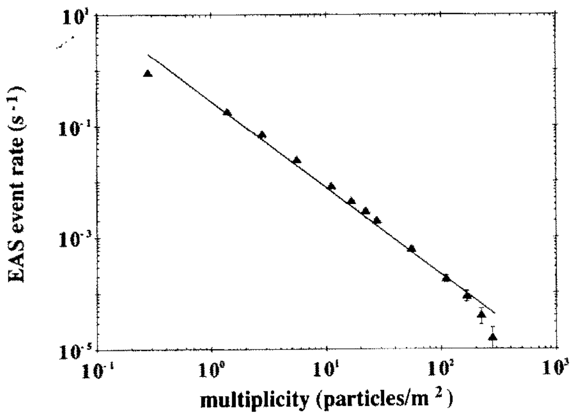

Fig. 11. Measured EAS rate.

As preliminary results, we show the measured EAS multiplicity rate in Fig. 11. The particle density Δ in the shower (number of charged particles per square meter) corresponds to the measured particle multiplicity in the top module. In the same figure we also report the best fit [22] (solid line) to the results of some cosmic-ray detectors obtained at sea level. The agreement is very good. In the low range of particle density, a small effect due to the trigger request of at least 10 particles in the bottom module can be observed. Particles with a low probability of interaction with the cryostat such as muons, and low-energy particles such as electrons, may not exceed the threshold of 10 particles in the bottom module. In the high range of density (more than 400–600 particles/m^2), the data are affected by ADC saturation.

Our results are not corrected for the effect due to the Laboratory height (260 m) and pressure variations. The best fit to our data give $H(>\Delta) = (0.354 \pm 0.006)\Delta^{(-1.55\pm0.01)}$ s^{-1}. The multiplicity rate measured in the bottom module when we require only one particle (corresponding to a detected charge ranging from 0.3 to 3.0 equivalent charged particles) and zero particles (corresponding to a value less

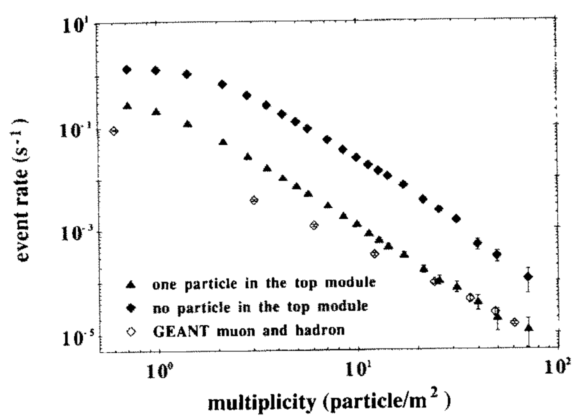

Fig. 12. Measured single particle rate in the bottom module.

then 0.3) in the top module is shown in Fig. 12.

Particles arriving at very large angles and not interacting with the antenna are included in this category. In the figure the total Monte Carlo prediction (for hadrons and muons) is shown for comparison. The experimental points are contaminated by background due to atmospheric showers. From this figure we can see that, with a reasonable offline cut (about 4 particle/m^2), the event rate is about 10^{-1} Hz. If we refer to Fig. 10 we see that with this kind of cut we have an efficiency of the order of 90% for hadrons losing more than 200 GeV in the bar. The efficiency for muons is clearly lower, due to the angular distribution that for high energy is peaked around the horizontal angle.

With a rate of events of $\simeq 10^{-1}$ Hz and a time resolution of the bar signal of the order of 100 ms [23], the dead time introduced in the NAUTILUS data taking is of the order of 10^{-2} s.

5. Conclusions

The first ultracryogenic gravitational wave antenna NAUTILUS is about to operate at an unprecedented sensitivity. The cosmic-ray detector assembled together with NAUTILUS has demonstrated a very good performance in the first data taking, well in agreement with the physics requirements of the experiment and with the simulation results. Despite the severe space constraints and a simple and cheap design, it amply fulfills the aim of detecting events in coincidence with the gravitational detector, even in the absence of calorimetric measurements.

Acknowledgements

We are very grateful to Prof. I. Modena and Prof. G. Pizzella for useful discussions. We also wish to thank A. Balla and G. Corradi for having designed and provided the Charge Walker modules and P. Benvenuto, D. Fabbri, M. Gatta and M. Ventura for their unlimited technical support.

References

[1] P. Astone et al., LNF-92/105(P), (1992).
[2] E. Iarocci. Nucl. Instr. and Meth. 217 (1983) 30.
[3] B.L. Beron and R. Hofstadter, Phys. Rev. 23 (1969) 148.
[4] B.L. Beron, S.P. Boughn, W.O. Hamilton, R. Hofstader and T.W. Martin, IEEE Trans. Nucl. Sci. NS-17 (1970) 65.
[5] A.M. Grassi Strini, G. Strini and G. Tagliaferri, J. Appl. Phys. 51(2) (1980).
[6] B.E. Moskowitz, Marcel Grossmann Meeting on General Relativity, (1986).
[7] E. Amaldi and G. Pizzella, Nuovo Cimento 9C (2) (1986).
[8] F. Ricci, Nucl. Instr. and Meth. A 260 (1987) 491.
[9] J. Chiang, P. Michelson and J. Price, Nucl. Instr. and Meth. A 311 (1992) 603.
[10] C. Bernard, A. De Rujula and B. Lautrup., Nucl. Phys. B 242 (1984) 93.
[11] G. Battistoni et al., Nuovo Cimento 9C (2) (1986) 653.

[12] M. Anelli et al., LNF-89/015(P) (1989).
[13] I. D'Antone et al., Sixth Conf. on Real-Time Computer Application in Nuclear, Particle and Plasma Physics, Real-Time 89, Williamsburg, Virginia, USA (1989).
[14] GEANT3 User Guide, CERN Data Holding Division DD/EE/84-1 (1987).
[15] G. Liu and B. Barish, Phys. Rev. Lett. 61-3 (1988).
[16] P. Astone et al., Phys. Rev. D 47-10 (1993).
[17] T.H.K. Barron, J.G. Collins and G.K. White, Adv. Phys. 29 (4) (1980) 609.
[18] F. Siohan, R.W. Ellsworth, M. LaPointe, J.R. MacFall, A. Stottlemyer and G.B. Yodh, J. Phys. G 3 (8) (1977).
[19] H. Arvela, M. Lumme, M. Nieminen, J. Peltonen, J.J. Torsti, E. Vainikka and E. Valtonen, J. Phys. G 10 (1984) 695.
[20] E.W. Cowan, K. Matthews, Phys. Rev. D 4 (1) (1971).
[21] A. Dar, Phys. Rev. Lett. 51 (1) (1983).
[22] J.B.T. Mc Caughan, J. Phys G 413 (1982).
[23] S. Frasca, Private communication.